Edge state in graphene ribbons: Nanometer size effect and edge shape dependence

Kyoko Nakada and Mitsutaka Fujita
Institute of Materials Science, University of Tsukuba, Tsukuba 305, Japan

Gene Dresselhaus and Mildred S. Dresselhaus
Massachusetts Institute of Technology, Cambridge, Massachusetts 02139-4307
(Received 26 June 1996)

Finite graphite systems having a zigzag edge exhibit a special edge state. The corresponding energy bands are almost flat at the Fermi level and thereby give a sharp peak in the density of states. The charge density in the edge state is strongly localized on the zigzag edge sites. No such localized state appears in graphite systems having an armchair edge. By utilizing the graphene ribbon model, we discuss the effect of the system size and edge shape on the special edge state. By varying the width of the graphene ribbons, we find that the nanometer size effect is crucial for determining the relative importance of the edge state. We also have extended the graphene ribbon to have edges of a general shape, which is defined as a mixture of zigzag and armchair sites. Examining the relative importance of the edge state for graphene ribbons with general edges, we find that a non-negligible edge state survives even in graphene ribbons with less developed zigzag edges. We demonstrate that such an edge shape with three or four zigzag sites per sequence is sufficient to show an edge state, when the system size is on a nanometer scale. The special characteristics of the edge state play a large role in determining the density of states near the Fermi level for graphite networks on a nanometer scale. [S0163-1829(96)11048-1]

I. INTRODUCTION

Graphite-related materials have long been a subject of interest. Recent attention has focused on porous carbons because of their large specific surface area (SSA). For example, some activated carbon fibers (ACF's) show extremely high SSA (up to 3000 m^2/g) corresponding to a high affinity for gas adsorption.[1] Materials having such high SSA's, with a huge exposed graphite surface, are good targets for applications, such as filters and capacitors. One of the most exciting current interests in porous carbons is as an alternative medium for high-capacity lithium ion batteries. [2]

In spite of the many possible applications of porous carbons, the basic understanding of the functionality of these materials has not yet been achieved. Even their structure is not clearly understood. For ACF's, nothing more than a simple structural model consisting of an assembly of minute graphite fragments has been proposed.[3] Each fragment is considered to have a size of 2–3 nm in plane and 3–4 turbostratically stacked layers, based on observed Raman spectra and x-ray diffraction measurements.[4] Tiny graphite fragments of a nanometer length are termed micrographites, which are believed to be the main components of porous carbons.

We cannot fully understand the functionality of these carbon materials without knowing the structure from a microscopic view, i.e., the structure as a network of sp^2 carbon fragments. Studies on fullerene molecules tell us that the topological structure of an sp^2 carbon network critically controls its π electronic structure and functionality as a material. In the closed cages of fullerene molecules, the relative arrangement of the 12 pentagonal rings, which act as pentagonal defects in the graphite network, generates a variety of π electronic states. Carbon nanotubes further demonstrate that the tubular circumferential vector (also called the chiral vector in the literature) critically controls whether the electronic state is metallic or insulating. These studies on π electron networks of nanometer dimensions show that the characteristic π electronic structure of carbon materials is essentially controlled by the network structure of sp^2 carbon, i.e., the topology of the mobile π electrons.

Some recent studies on carbon nanotubes[5,6] also suggest that there might exist a new kind of nanotube. The newly proposed structural model is not simply a cylindrical form, as the ordinary nanotube is considered to be, but a quite defective form having a lot of edge dislocations. It should be noted that these nanotubes may also have other defects in their π electron networks. One such defect is an *edge*. In cylindrical tubules, carbon atoms all bond to three neighboring carbons as in a graphite sheet. Defective nanotubes, however, may have some edge sites where there are only two neighboring carbons. Since the mobile π electrons are situated in topologically different circumstances at edge sites, their π electronic states may be affected significantly.

The existence of defective nanotubes introduces a new category of π electronic systems which may also be applicable to some porous carbons, i.e., nanometer-sized graphite fragments with edges. The precise structure of porous carbons is far from being understood at present, because of their high degree of disorder. Porous carbons may have dangling bonds, sp^3 bonded carbons, and functional groups, all affecting their functionality. However, they also have some nanoscale regions where the crystal structure of graphite is well developed. We thus propose that porous carbons may have many edge sites on the periphery of their micrographite constituents.

Our attention in the present work focuses on nanometer-scale π electronic systems which are confined by edges.

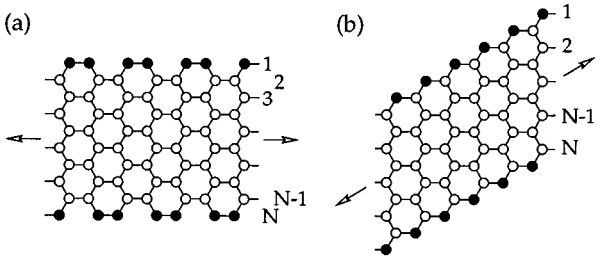

FIG. 1. The network skeleton of an armchair ribbon ($N=10$) (a) and a zigzag ribbon ($N=5$). (b) The edge sites are indicated by solid circles on each side. Periodic boundary conditions are assumed for the edges. The arrows indicate the translational directions of the graphene ribbons.

Such graphite networks may have an electronic structure which is somewhat different from that of bulk graphite, since quite a large fraction of the carbon atoms sit on the edge.

There are two basic shapes for graphite edges, namely, armchair and zigzag edges. Some theoretical work[7–11] on the electronic structure of finite-sized graphite systems, either as molecules or as one-dimensional systems, has shown that graphite networks with zigzag edges have a localized *edge state* at the Fermi level, but those with armchair edges have no such state. The edge structure of a real micrographite fragment is naturally considered to be more irregular and complicated. The main purpose of this paper is to examine whether or not the edge state survives in finite-sized graphite structures with general edge shapes, where the edges can be described as mixtures of both armchair and zigzag sites. To study the relationship between the π electronic structure and the edge shape, we consider a series of one-dimensional graphene ribbons systematically, as a function of the edge shape. By examining the electronic structure of graphene ribbons of different widths, we obtain the size effect of the edge state on a nanometer scale.

The electronic structure of graphene ribbons having armchair and zigzag edges is reviewed in Sec. II, emphasizing the mathematical nature of the edge state. In Sec. III, we develop the electronic structure of graphene ribbons with general edge shapes, giving special emphasis to the size effect on a nanometer scale. Section IV is devoted to discussions of the edge state in graphene ribbons.

II. GRAPHENE RIBBONS WITH ARMCHAIR AND ZIGZAG EDGES

In this section we review the electronic structure of graphene ribbons with armchair and zigzag edges. We can cut a graphene sheet along a straight line as shown in Fig. 1 to illustrate the two prototype edge shapes, namely, the armchair edge [Fig. 1(a)] and the zigzag edge [Fig. 1(b)] with a difference of 30° in the axial direction between the two edge orientations. Figure 1 thus shows the two basic graphene ribbons which are defined as one-dimensional graphite networks confined by a pair of parallel armchair (zigzag) edges on both sides.

The ribbon width N denotes the number of dimer lines for armchair ribbons and the number of zigzag lines for zigzag ribbons. The edge sites are emphasized by solid circles on each side. Throughout this paper, the dangling bonds on the edge sites are all assumed to be terminated by hydrogen atoms, and the dangling bonds make no contribution to the electronic state near the Fermi level.

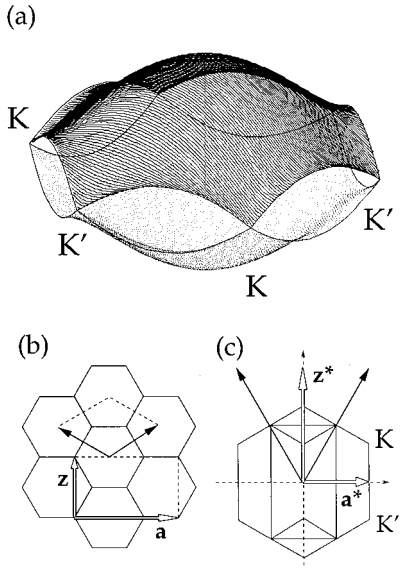

FIG. 2. Energy band structure (a) and unit cells in real space (b) and reciprocal space (c) of 2D graphite. The vectors **a** and **a*** (**z** and **z***) relate to armchair (zigzag) ribbons (see text) in (b) and (c). The valence and conduction bands make contact at the degeneracy point K.

To calculate the electronic states for the ribbon, we employ a tight-binding band calculation within the Hückel approximation, in order to focus our attention on the relationship between the π electronic structure and the edge shape. Transfer integrals between the nearest-neighbor sites are all set at t for simplicity. Although electron-electron and electron-phonon interactions are also important in real systems, we do not consider these interactions in the present work, since we aim here to reveal the intrinsic difference in the π electronic state originating from the topological nature of the various ribbon edges.

We start with the band structure of a two-dimensional (2D) graphite sheet, since the corresponding band structure of graphene ribbons can be predicted from that of the 2D graphite sheet, which is a zero gap semiconductor, as shown in Fig. 2(a). The upper and lower bands are degenerate at a single point K in the Brillouin zone (BZ), and at each K point, the electronic bands $E(k)$ show a linear k dispersion relation. The real and reciprocal spaces of 2D graphite are depicted in Figs. 2(b) and 2(c). Taking a rectangular real space unit cell, as shown in Fig. 2(b), makes the BZ fold into a rectangle, which is half as large as the hexagonal BZ shown in Fig. 2 (c). The unit vector **a** (**z**) denotes the translational axis of an armchair (zigzag) ribbon, and the shorter (longer) side of the rectangular BZ is the one-dimensional BZ of armchair (zigzag) ribbons. The global band structure of graphene ribbons having armchair (zigzag) edges is then predicted by projecting that of 2D graphite onto the corresponding axis **a*** (**z***) using the zone-folding technique. The linear dispersion relations stemming from the original K

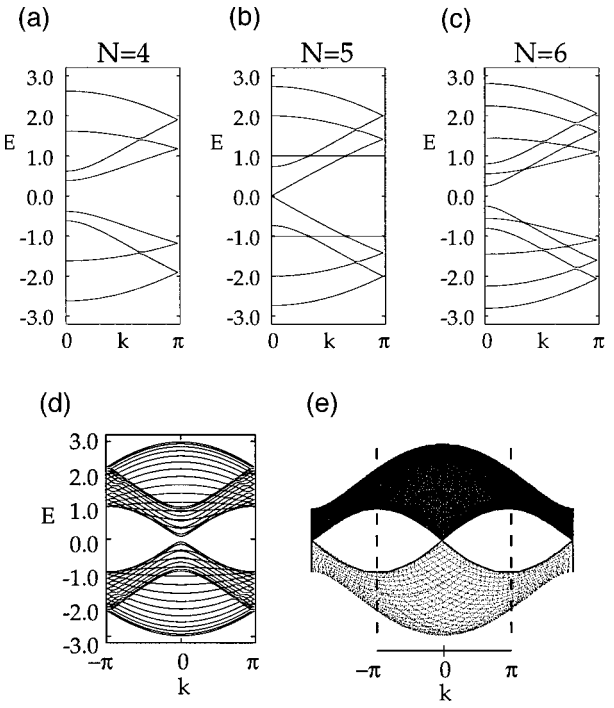

FIG. 3. Calculated band structure $E(k)$ of armchair ribbons of various widths [$N=4$ (a), 5 (b), and 6 (c)], calculated band structure of an armchair ribbon of $N=30$ (d), and the projected band structure of 2D graphite onto an armchair axis (e). Dashed lines in (e) indicate the boundary of the first BZ where the zone-folding technique should be applied.

point are expected to appear around $k=0$ ($|k|=2\pi/3$) for armchair (zigzag) ribbons.

The calculated band structures of armchair ribbons are shown in Figs. 3(a)–3(c), for three different ribbon widths. The wave number k is normalized by the primitive translation vector of each graphene ribbon, and the energy E is scaled by the transfer integral t throughout this paper. The top of the valence band and the bottom of the conduction band are located at $k=0$, as expected. It is interesting to note that the ribbon width critically controls whether the system is metallic or insulating. As shown in Fig. 3(b), the system is metallic when $N=3M-1$, where M is an integer. This periodicity can be mathematically understood by regarding the system at $k=0$ as a ladder network,[12] and the wave function is obtained analytically.[11] For the insulating ribbons, the direct gap decreases with increasing ribbon width and tends to zero in the limit of very large N. In Fig. 3(d), we show the calculated band structure of an armchair ribbon ($N=30$) together with the band structure of 2D graphite projected onto an armchair axis [Fig. 3(e)]. It is seen that the projected band structure of 2D graphite is almost reproduced by that of a wide armchair ribbon.

For zigzag ribbons, however, a remarkable new feature arises in the band structure, as shown in Figs. 4(a)–4(c). Here we see that the highest valence band state and the lowest conduction band state for the zigzag ribbons are always degenerate at $k=\pi$, though the degeneracy is expected to appear at $|k|=2\pi/3$ on the basis of the projected band structure of 2D graphite. We find that the degeneracy of the center

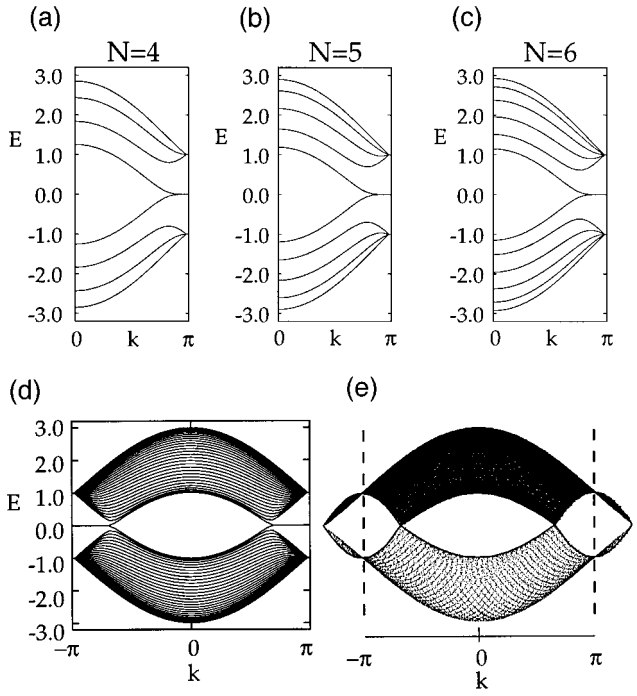

FIG. 4. Calculated band structures $E(k)$ of zigzag ribbons [$N=4$ (a), $N=5$ (b), and $N=6$ (c)], calculated band structure of a zigzag ribbon (d), and the projected band structure of 2D graphite onto a zigzag axis (e). See the caption of Fig. 3.

bands at $k=\pi$ does not originate from the intrinsic band structure of 2D graphite, and the corresponding wave functions are completely localized on the edge sites. These two special center bands get flatter with increasing ribbon width. We show the band structure for the zigzag ribbon ($N=30$) together with the projected band structure of 2D graphite in Figs. 4(d) and 4(e). A pair of almost flat bands appears within the region of $2\pi/3\leqslant|k|\leqslant\pi$ where the bands sit in the very vicinity of the Fermi level. No such flat band is expected for the projected band structure of 2D graphite. As seen in Fig. 4(d) the second lowest conduction band shows a dip near $|k|=2\pi/3$, where the highest valence band below the center bands shows a rise, approaching closer to each other as N increases, thereby reproducing the electronic state around the original K point in 2D graphite.

By examining the charge density distribution, we find that the electronic states in the almost flat bands correspond to a state localized on the zigzag edge.[10,13] We then derive an analytic expression for the electronic wave functions for the edge state by considering a semi-infinite graphene sheet with a zigzag edge.[11] The analytic form of the wave function is depicted in Fig. 5.

Considering the translational symmetry, we can start constructing the analytic solution for the edge state by letting the Bloch components of the linear combination of atomic orbitals (LCAO) wave function be $\ldots,e^{ik(n-1)},e^{ikn},e^{ik(n+1)},\ldots$ on successive edge sites, where n denotes a site location on the edge. Then the mathematical condition necessary for the wave function to be exact for $E=0$ is that the total sum of the components of the complex wave function over the nearest-neighbor sites should vanish. In Fig. 5, the above condition is as follows:

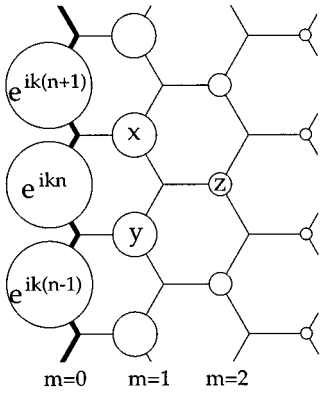

FIG. 5. An analytic form of the edge state for a semi-infinite graphene sheet with a zigzag edge, which is emphasized by bold lines. Each carbon site is specified by a location index n on the zigzag chain and by a chain order index m from the edge. The magnitude of the charge density at each site, such as x, y, and z, is obtained analytically (see text). The radius of each circle is proportional to the charge density on each site, and the drawing is made for $k=7\pi/9$.

$e^{ik(n+1)}+e^{ikn}+x=0$, $e^{ikn}+e^{ik(n-1)}+y=0$, and $x+y+z=0$. Therefore, the wave function components x, y, and z are found to be $[-2\cos(k/2)]e^{ik(n+1/2)}$, $[-2\cos(k/2)]e^{ik(n-1/2)}$, and $[-2\cos(k/2)]^2e^{ikn}$, respectively. We can thus see that the charge density is proportional to $[2\cos(k/2)]^{2m}$ at each non-nodal site of the mth zigzag chain from the edge. Then the convergence condition of $|-2\cos(k/2)|\leq 1$ is required, for otherwise the wave function would diverge in a semi-infinite graphene sheet. This convergence condition defines the region $2\pi/3\leq|k|\leq\pi$ where the flat band exists. Now we can see that the resultant nonbonding orbital is a wave function, which penetrates from the edge sites to the inner sites, decaying by a damping factor of $-2\cos(k/2)$ per zigzag chain. In Fig. 5, the radius of each circle is proportional to the charge density, and the drawing is made for $k=7\pi/9$. The edge state of a semi-infinite graphene sheet is a special state that analytically connects the localized state at $k=\pi$ and the delocalized state at $|k|=2\pi/3$, which is nothing but the electronic state of 2D graphite at the Fermi level.

III. GRAPHENE RIBBONS WITH GENERAL EDGES

We demonstrated in the previous section that zigzag ribbons show a localized edge state at the Fermi level. Considering a semi-infinite graphene sheet with a zigzag edge, we showed the mathematical features of the edge state. In this section we show how the edge state affects the electronic structure of real nanoscale graphite systems, such as those occurring in porous carbons. Since those real graphite systems have a rather complicated structure, we have to consider many factors which could affect the properties of the edge state. In the following subsections we discuss the significant parameters which control the properties of the edge state, i.e., the system size and edge shape surrounding the graphite network. We first examine the size dependence of the edge state by taking the ribbon width as a size parameter,

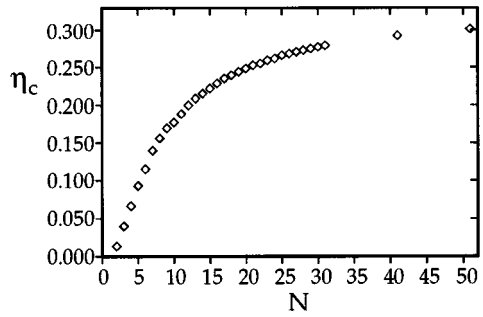

FIG. 6. The flatness index for the center bands η_c of a zigzag ribbon vs the ribbon width N. The flatness index approaches a maximum of 1/3 as N goes to infinity.

and then examine the edge-shape effect by considering the graphene ribbon to have a general edge shape which is defined as a mixture of zigzag and armchair sites.

A. Size dependence on the edge state

In a semi-infinite graphene sheet with a zigzag edge, a perfectly flat energy band appears in the range of $2\pi/3\leq|k|\leq\pi$. The wave function is entirely localized at $k=\pi$, but it penetrates into the inner sites, as k shifts away from π. In zigzag ribbons, the wave function penetration from both edges results in a small gap in the range of $2\pi/3\leq|k|<\pi$. Since an infinitesimal k deviation from π can make a gap, no flat band exists in the strict sense. The penetrating wave function, however, decays exponentially on successive inner zigzag chains. The magnitude of the gap at a specific k point therefore depends on the ribbon width. As shown in Fig. 4, the wider the ribbon, the larger the range of k values over which the bands are almost flat.

The almost flat bands near the Fermi level are expected to give rise to a remarkably sharp peak in the density of states, where the charge density is extremely localized on the edge sites. It should be noted, however, that only the pair of center bands contribute to the localized state, and only in the region of $2\pi/3\leq|k|\leq\pi$. All of the other $2N-2$ bands, except for the two center bands, tend to reproduce the band structure of 2D graphite, as projected onto the zigzag direction. The importance of the edge state should thus be measured in a normalized way.

We quantitatively evaluate the relative magnitude of the edge state by introducing the flatness index η_c and η_a, defined as $\eta_c=n_{E\approx0}/n_c$ and $\eta_a=n_{E\approx0}/n_a$, where $n_{E\approx0}$ is the number of the states with $E\approx0$ and n_c (n_a) is the total number of states in the center (all) bands. In Fig. 6, the flatness index for the pair of center bands η_c is plotted for zigzag ribbons having various widths. In computing η_c and η_a, the electronic states with $|E|\leq0.002$ are treated as $E\approx0$. The flatness index η_c monotonically increases as the ribbon gets wider. It is expected that η_c will converge to 1/3, corresponding to the range of $2\pi/3\leq|k|\leq\pi$ where a perfectly flat band appears in the first BZ of a semi-infinite graphene sheet.

We next plot the flatness index for all the bands η_a to evaluate the relative importance of the edge state within the total electronic structure of a zigzag ribbon (Fig. 7). The

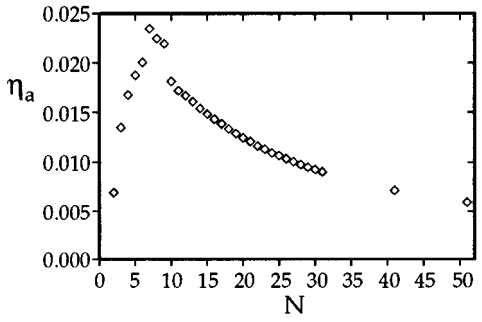

FIG. 7. The flatness index for all the bands η_a vs ribbon width N.

flatness index η_a increases at first, corresponding to the increase in η_c. The flatness index η_a reaches a maximum around $N=7$, where the zigzag ribbon is about 1.3 nm wide, and diminishes after that with further increase in N. The rate of the decrease is approximately proportional to $1/N$. We can thus see that the significance of the special edge state disappears in a graphene sheet where the ribbon width becomes infinitely large. This ensures the continuity of our model from the finite graphene ribbons to a 2D graphite sheet. When the ribbon width is about a few nm, however, approximately 2% of the total number of π electronic states is concentrated in the vicinity of $E=0$.

The localized states make a remarkably sharp peak in the density of states near the Fermi level, because the intrinsic band structure of 2D graphite has only a very few states near the Fermi level. In Fig. 8, the density of states of the zigzag ribbons ($N=6$, 11, and 51) are depicted. The corresponding ribbon widths are about 1.1, 2.2, and 10.6 nm, respectively. It is clear from Fig. 8 that the relative importance of the edge state strongly depends on the ribbon width. The edge state is very important when the ribbon width is of nanoscale size. Even for a ribbon of about 10 nm width ($N=51$), a non-negligible peak in the density of states is observed [see Fig. 8(c)], which is comparable to the van Hove singularity at $E=\pm 3.0$. The weight of the edge state in the normalized density of states, however, diminishes proportionally to $1/N$ when the ribbon extends to even larger N values. This demonstrates that nanoscale graphite fragments can show singular electronic states at the Fermi level through the presence of zigzag sites, giving rise to an effect that is not present in bulk graphite at all.

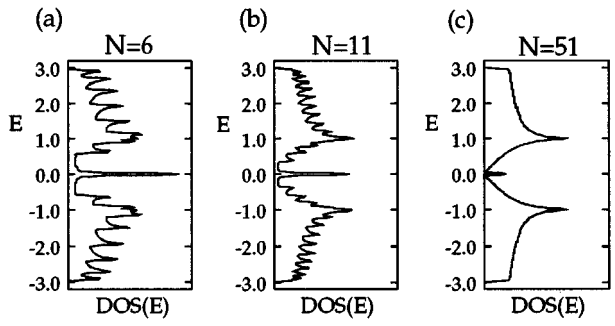

FIG. 8. Density of states (DOS) of zigzag ribbons of different widths: (a) $N=6$, (b) $N=11$, and (c) $N=51$.

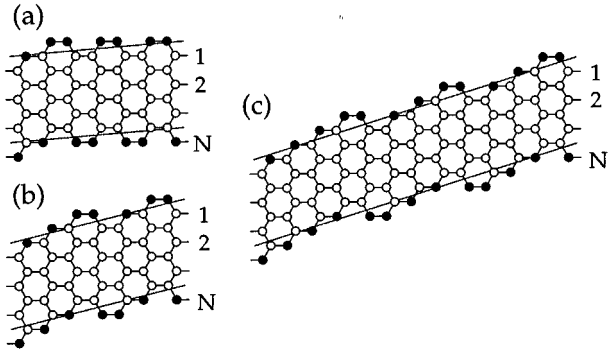

FIG. 9. The unit cells and edge vectors of general ribbons. The edge sites are denoted by solid circles, and the corresponding zigzag ratio r_{zig} is (a) 0.25, (b) 0.60, and (c) 0.70 (see text).

B. Effect of edge shape

As demonstrated in the previous section, zigzag ribbons of a nanoscale size show a singular edge state at the Fermi level. On the other hand, armchair ribbons with a difference of 30° in the axial direction have no such localized state at all. The edge structure in a real micrographite is naturally rather irregular and complicated. It is therefore important to investigate the conditions under which the edge state survives for more realistic edge terminations. To analyze the relationships between the edge shape and the electronic state in a more practical model, we next examine the electronic structure of graphene ribbons having more general edge shapes, which can be represented as a mixture of zigzag and armchair sites.

Our model for a general graphene ribbon is described by a pair of parallel edge vectors, which connect identical carbon rings on each edge, and the unit cell exhibits translational symmetry. The unit cells of some general ribbons, defined in accordance with this model, are depicted together with a pair of edge vectors in Fig. 9. This pair of edge vectors forms a parallelogram, and those hexagons whose centers are located inside the parallelogram constitute the unit cell of the graphene ribbon. The axial direction of an edge vector determines the edge shape, and the distance between the edge vectors determines the ribbon width, which parametrizes the size factor of the finite graphite systems.

By varying the direction of the edge vector from 0° (armchair) to 30° (zigzag), we examine systematically whether and how the edge state survives in general graphene ribbons. To specify the edge shape, let us define the zigzag ratio r_{zig} as the number of the zigzag sites relative to the total number of the edge sites. As seen in Fig. 1, the armchair edge is specified by a pair of sequential edge sites lying in between the threefold-coordinated sites, and the zigzag edge is specified by a single edge site enclosed by a pair of threefold-coordinated sites. Denoting an armchair (zigzag) site by the letter a (z), we can express the edge structure of a graphene ribbon by a permutation of a and z. In Fig. 9, the edge sites are emphasized by solid circles. The edge structure

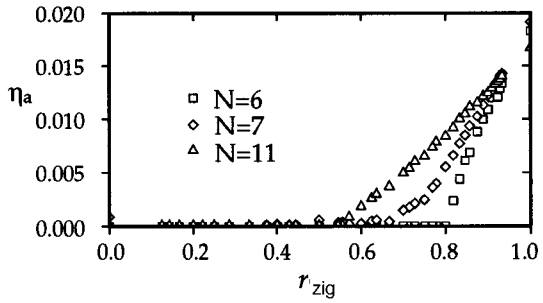

FIG. 10. The flatness index for the total bands η_a vs zigzag ratio r_{zig} for general ribbons of $N=6,7,11$.

is expressed as (a) *zaaa*, (b) *zzaza*, and (c) *zzzazzazza*, and the corresponding zigzag ratio r_{zig} is therefore (a) 0.25, (b) 0.60, and (c) 0.70.

In Fig. 10, the flatness index for the total bands η_a is plotted versus the zigzag ratio r_{zig} for general ribbons of $N=6,7,11$, showing that η_a for the total band structure depends on r_{zig}. It is clear that the insertion of armchair sites into a zigzag edge directly reduces η_a for the total band structure, since the armchair edge makes no contribution to the flat band state. The tail seen in the $N=7$ plot below $r_{\mathrm{zig}}\approx 0.7$ is considered to be influenced by the metallic armchair ribbon of that width. The flatness index for the total band structure η_a also depends on the ribbon width. In the relatively narrow ribbons ($N=6$), η_a rapidly decreases with decreasing r_{zig}, and those ribbons with $r_{\mathrm{zig}}\leqslant 0.8$ show no state with $E\approx 0$. In the wider ribbons, however, η_a decreases more slowly. We can see in Fig. 10 that even those ribbons having more than 1/3 of their edge sites as armchair sites show enough flatness to cause a notable edge state, if they have a ribbon width $N\approx 10$, i.e., a ribbon width of a few nm.

In the present scheme for generating a general edge structure by introducing a pair of edge vectors, each armchair site is inserted rather uniformly. The zigzag ratio r_{zig} therefore has the following relation to the average number of sequential zigzag sites $\mathrm{seq}_{\mathrm{zig}}$:

$$1/\mathrm{seq}_{\mathrm{zig}}=[1/r_{\mathrm{zig}}]-1. \tag{1}$$

In Fig. 11, the flatness index for the total band structure η_a is plotted versus $\mathrm{seq}_{\mathrm{zig}}$. It is seen that only three or four zigzag sites in a sequence are enough to show a non-negligible edge state, when the ribbon is a few nm in width. As an example, we depict the unit cell of a graphene ribbon with $N=11$ [Fig. 12(a)] and the corresponding density of states [Fig. 12(b)]. The zigzag sites are emphasized by solid circles in Fig. 12(a), and the sequences of zigzag sites are interrupted by armchair sites, so that the ribbon in Fig. 12(a) has at most three zigzag sites in a sequence, which may be representative of real micrographite fragments. As seen in Fig. 12(b), however, the ribbon shows a non-negligible peak in the density of states at the Fermi level.

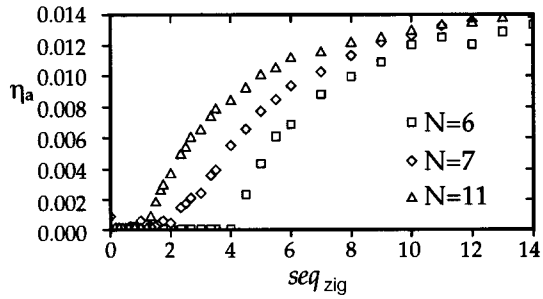

FIG. 11. The flatness index for all the bands η_a vs the average number of sequential zigzag sites $\mathrm{seq}_{\mathrm{zig}}$ for general ribbons of $N=6,7,11$.

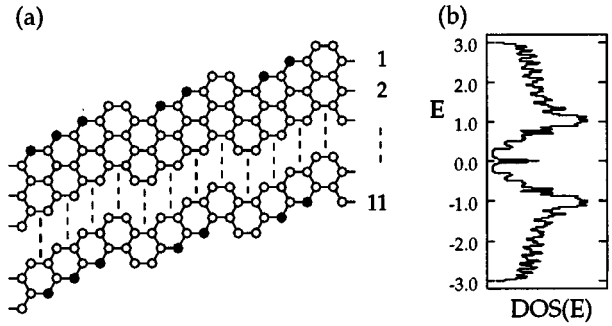

FIG. 12. (a) The unit cell of a general graphene ribbon of $N=11$. The zigzag sites are indicated by solid circles. (b) The corresponding density of states (DOS). The edge state is observed as a non-negligible peak in the DOS at the Fermi level.

C. Localization of wave functions

Let us now discuss an important feature of the edge state, namely, the localization of the wave function. We see from Fig. 5 that the wave function in the edge state is mostly localized on the edge sites. Our next interest is whether and how the localized wave function survives in graphene ribbons having general edge shapes. We examine the net charge density in the edge state, i.e., the charge density distribution in the electronic states with $|E|\leqslant 0.002$. We then find that the charge density in the edge state is strongly localized on the zigzag sites even for the graphene ribbons having small zigzag sequences fragmented by armchair sites. In Fig. 13, the maximum charge density in the edge state at a zigzag site is plotted versus the average number of sequential zigzag sites $[\mathrm{seq}_{\mathrm{zig}}]$ for graphene ribbons with $N=6$ and $N=11$. The

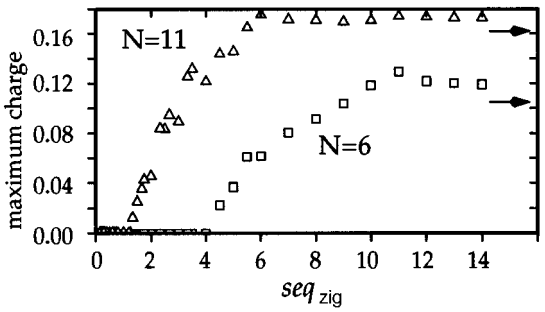

FIG. 13. The maximum charge density on the zigzag sites vs the average number of sequential zigzag sites $\mathrm{seq}_{\mathrm{zig}}$ for graphene ribbons of $N=6,11$. The arrows indicate the corresponding value for pure zigzag ribbons.

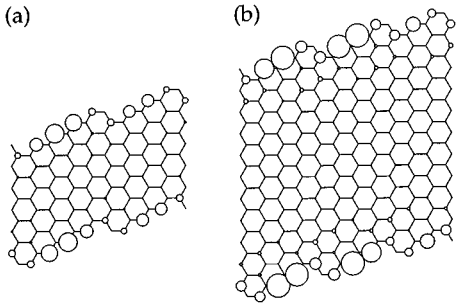

FIG. 14. Charge density distribution in the edge state, where the electronic states with $|E| \leq 0.02$ are regarded as belonging to the edge state.

arrows show the corresponding value for the pure zigzag ribbons with $N=6$ and $N=11$. The maximum charge density for both ribbons overshoot the corresponding pure zigzag value, but this is due to the numerical method we employed. When the system size is relatively small ($N=6$), graphene ribbons having less than four zigzag sites in a sequence have no edge state with $E \approx 0$. The wider graphene ribbons ($N=11$ and 2.5 nm in width) with the same edge shape can show some edge state, where the charge density is fairly localized on the zigzag sites. From Fig. 13, we can see that four or five zigzag sites per sequence are enough to exhibit an edge state for graphene ribbons on a nanometer scale. It is also demonstrated that in the edge state with $E \approx 0$ a net charge of more than 0.1 per zigzag site is localized on the zigzag sites, which may be detected experimentally by techniques such as scanning tunnel microscopy (STM).

In the above discussions, the criterion of $|E| \leq 0.002$ works well to tell whether or not the electronic state is to be regarded as $E \approx 0$. In connection with experimental measurements such as those using the STM technique, however, electronic states over a much wider range will inevitably be observed together. We therefore depict in Fig. 14 the net charge density in the edge state, where the electronic states with $|E| \leq 0.02$ are treated as part of the edge state. In this figure, it is demonstrated that these graphene ribbons show a strongly localized charge density distribution on the zigzag sites, in spite of the deficiency of a well-developed zigzag edge. It is also expected that the localized charge density shown in Fig. 14 could be detected in real graphite materials, such as porous carbons.

IV. DISCUSSION

In the present paper we studied systematically the π electronic structure of nanometer-scaled graphite networks utilizing the model of graphene ribbons with various edge shapes. We first showed the mathematical feature of the edge state, which is seen as special localized states near the Fermi level in the graphite networks with a zigzag edge. The edge state stems not from bulk graphite nor the dangling bonds, but from the topology of the π electron networks with a zigzag edge. The graphite networks with an armchair edge, the other prototype edge shape of graphite, also exhibit no such localized state. We thus studied the π electronic structure of graphene ribbons having various edge vectors and ribbon widths, which are treated as parameters specifying the edge shape and system size, respectively. Examining the relative magnitude of the edge state, we find that a non-negligible edge state still survives in graphene ribbons with less developed zigzag edges. It is remarkable to note that only three or four zigzag sites per sequence are enough to show an edge state in these graphene ribbons. The size effect of the edge state is of great significance, since the relative importance of the edge state should vanish in bulk graphite. From the discussion regarding Fig. 7, zigzag ribbons with $N \approx 10^4$ are expected to show a flatness index for the total band structure η_a which is about 1/100 as large as that for the $N=51$ ribbon. Ribbons with $N \approx 10^4$ are ~ 2.4 μm in width. We thus conclude that graphite networks of a nanometer length are the best candidates to exhibit the special edge state.

Among the many carbon materials of interest, those such as porous carbons, which are considered to be made up from micrographites, are particularly interesting, since they may have a lot of edge sites on the periphery of their micrographite constituents. As we demonstrated, the mathematically pure zigzag edge is not necessarily required to show an edge state. Less developed edges with three or four zigzag sites per sequence are enough to exhibit a non-negligible edge state. It is naturally supposed that some of the micrographites in a real system may have such edge structures, where a strongly localized charge density distribution such as shown in Fig. 14 is expected.

Because of the quite disordered structure of candidate carbon systems such as porous carbons, measurements of their electronic properties have not yet been fully carried out. Some interesting observations of their electronic and magnetic properties are strongly related to their dangling bonds or metal impurities. However, we propose an additional possibility that the π electrons by themselves can also exhibit a special electronic state near the Fermi level, which may affect the electronic properties. The edge state, stemming from the topology of the π electron networks, may be observed as states localized on the edge sites by some experimental techniques, if the microscopic structure is well described by π electron systems on a nanometer scale.

ACKNOWLEDGMENTS

The authors are grateful to Dr. K. Kusakabe of Institute for Solid State Physics, and K. Wakabayashi of University of Tsukuba, for their collaboration, numerous discussions, and some figures. Fruitful discussions with Professor T. Enoki of Tokyo Institute of Technology, and Dr. A. Nakayama of National Institute of Materials and Chemical Research are gratefully acknowledged. The authors would like to thank Professor M. Endo of Shinshu University, Professor K. Kaneko of Chiba University, M. J. Matthews of Massachusetts Institute of Technology, and Professor H. Hosoya of Ochanomizu University, for their helpful suggestions. One of the authors (K.N.) acknowledges support from Japan Society for the Promotion of Science. K.N. is also indebted to Y. Satomi for the algorithm to generate graphene ribbons with general edges. This work is partly supported by NSF Grant No. DMR 95-10093 (M.S.D.) and by a Grant-in-Aid for Scientific Research from the Ministry of Education, Science and Culture, Japan (M.F.).

[1] K. Tai and N. Shindo, Polym. Process. **35**, 384 (1986).
[2] K. Sato, M. Noguchi, A. Demachi, N. Oki, and M. Endo, Science **264**, 556 (1994).
[3] K. Kaneko, C. Ishii, M. Ruike, and H. Kuwabara, Carbon **30**, 1075 (1991).
[4] A. M. Rao, A. W. P. Fung, M. S. Dresselhaus, G. Dresselhaus, and M. Endo, J. Mater. Res. **7**, 1788 (1992).
[5] O. Zhou, R. M. Fleming, D. W. Murphy, R. C. Haddon, A. P. Ramirez, and S. H. Glarum, Science **263**, 1744 (1994).
[6] S. Amelinckx, D. Bernaerts, X. B. Zhang, G. Van Tendeloo, and J. Van Landuyt, Science **267**, 1334 (1995).
[7] S. E. Stein and R. L. Brown, J. Am. Chem. Soc. **109**, 3721 (1987).
[8] H. Hosoya, Y.-D. Gao, K. Nakada, and M. Ohuchi, in *New Functionality Materials*, edited by C. T. Tsuruta, M. Doyama, and M. Seno (Elsevier, New York, 1993), p. 27.
[9] K. Tanaka, S. Yamashita, H. Yamabe, and T. Yamabe, Synth. Met. **17**, 143 (1987).
[10] M. Fujita, M. Yoshida, and K. Nakada, Fullerene Sci. Technol. **4**, 565 (1996).
[11] M. Fujita, K. Wakabayashi, K. Nakada, and K. Kusakabe, J. Phys. Soc. Jpn. **65**, 1920 (1996).
[12] H. Hosoya, H. Kumazaki, K. Chida, M. Ohuchi, and Y.-D. Gao, Pure Appl. Chem. **62**, 445 (1990).
[13] K. Kobayashi, Phys. Rev. B **48**, 1757 (1993).